

## In Ga N Ga N nanostripe grown on pattern sapphire by metal organic chemical vapor deposition

T. S. Ko, T. C. Wang, R. C. Gao, Y. J. Lee, T. C. Lu, H. C. Kuo, S. C. Wang, and H. G. Chen

Citation: [Applied Physics Letters](#) **90**, 013110 (2007); doi: 10.1063/1.2430487

View online: <http://dx.doi.org/10.1063/1.2430487>

View Table of Contents: <http://scitation.aip.org/content/aip/journal/apl/90/1?ver=pdfcov>

Published by the [AIP Publishing](#)

---

### Articles you may be interested in

[Correlating exciton localization with compositional fluctuations in In Ga N Ga N quantum wells grown on GaN planar surfaces and facets of GaN triangular prisms](#)

*J. Appl. Phys.* **102**, 093502 (2007); 10.1063/1.2802291

[Radiative and nonradiative lifetimes in nonpolar m -plane In x Ga 1 - x N Ga N multiple quantum wells grown on GaN templates prepared by lateral epitaxial overgrowth](#)

*J. Vac. Sci. Technol. B* **25**, 1524 (2007); 10.1116/1.2746354

[Growth of InP self-assembled quantum dots on strained and strain-relaxed In x \( Al 0.6 Ga 0.4 \) 1 - x P matrices by metal-organic chemical vapor deposition](#)

*J. Appl. Phys.* **100**, 043511 (2006); 10.1063/1.2244519

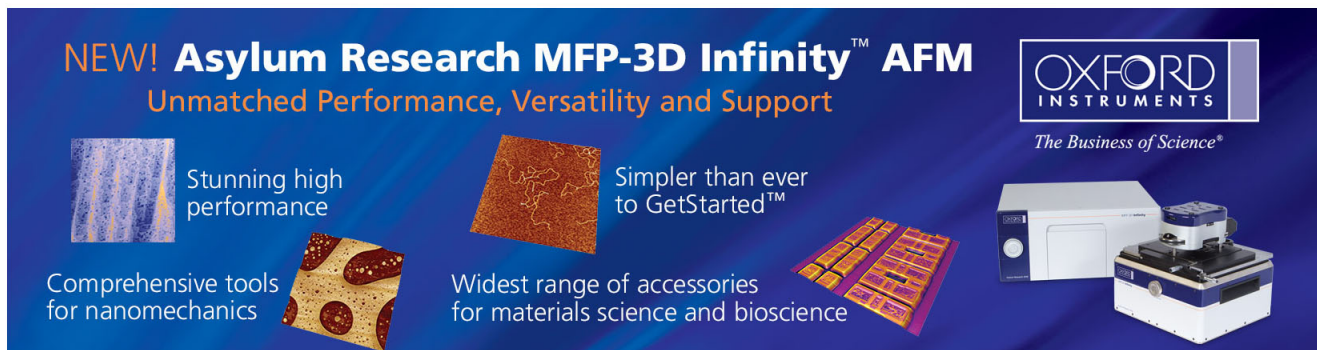
[Superlattice-like stacking fault and phase separation of In x Ga 1x N grown on sapphire substrate by metalorganic chemical vapor deposition](#)

*Appl. Phys. Lett.* **77**, 247 (2000); 10.1063/1.126939

[Phase separation and ordering coexisting in In x Ga 1x N grown by metal organic chemical vapor deposition](#)

*Appl. Phys. Lett.* **75**, 2202 (1999); 10.1063/1.124964

---



**NEW! Asylum Research MFP-3D Infinity™ AFM**  
Unmatched Performance, Versatility and Support

**OXFORD INSTRUMENTS**  
*The Business of Science®*

Stunning high performance

Simpler than ever to GetStarted™

Comprehensive tools for nanomechanics

Widest range of accessories for materials science and bioscience

*Asylum Research*

## InGaN/GaN nanostripe grown on pattern sapphire by metal organic chemical vapor deposition

T. S. Ko, T. C. Wang, R. C. Gao, Y. J. Lee, T. C. Lu,<sup>a)</sup> H. C. Kuo,<sup>b)</sup> and S. C. Wang  
*Department of Photonics and Institute of Electro-Optical Engineering, National Chiao Tung University,  
 1001 Ta Hsueh Rd., Hsinchu 30050, Taiwan, Republic of China*

H. G. Chen

*Department of Materials Science and Engineering, I-Shou University, Kaohsiung 840, Taiwan,  
 Republic of China*

(Received 4 October 2006; accepted 5 December 2006; published online 4 January 2007)

The authors have used metal organic chemical vapor deposition to grow InGaN/GaN multiple quantum well (MQW) nanostripes on trapezoidally patterned *c*-plane sapphire substrates. Transmission electron microscopy (TEM) images clearly revealed that the MQWs grew not only on the top faces of the trapezoids but also on both lateral side facets along the [0001] direction defined by the selected area electron diffraction pattern. Meanwhile, dislocations that stretched from the interfaces between the GaN and the substrates did not pass through the MQWs in the TEM observation. Microphotoluminescence measurements verified that the luminescence efficiency from a single nanostripe was enhanced by up to fivefold relative to those of regular thin film MQW structures. Observation of the cathodoluminescence identified the areas of light emission and confirmed that enhanced emission occurred from the nanostripes. © 2007 American Institute of Physics. [DOI: 10.1063/1.2430487]

Group III nitride semiconductors attract much attention because of their applications in light emitting devices such as highly efficient light emitting diodes (LEDs) and laser diodes.<sup>1,2</sup> Although such LEDs are commercially available, it is difficult to manufacture highly efficient LEDs because a great number of threading dislocation densities occur when group III nitride alloys are grown on *c*-plane sapphire.<sup>3</sup> Moreover, most of the light emitted from the LED active region would remain trapped by the high refractive index of GaN as a result of total internal reflection at the interface between the LED and air.<sup>4,5</sup> Recently, Kim *et al.* demonstrated high-efficiency LEDs from dislocation-free InGaN/GaN multiple quantum well (MQW) nanorod arrays prepared using a metal organic chemical vapor deposition (MOCVD) system.<sup>6</sup> Fujii *et al.* improved the luminescence efficiency of LEDs by roughening the sample surface to enlarge the emission area.<sup>7</sup> Wang *et al.* fabricated a micropillar InGaN/Cu LED combining a patterned sapphire substrate.<sup>8</sup> From these previous studies, it is clearly most desirable to grow InGaN/GaN heterostructures that have low dislocation densities and large surface areas in order to increase the emission efficiency. Nanostructure devices could play an important role in overcoming the existing dislocations and difficulties encountered in light extraction. In this letter, we describe high-efficiency InGaN/GaN MQWs embedded in nanostripe structures prepared through MOCVD growth on *c*-plane sapphire substrates patterned with trapezoid stripes. The structural analysis of these materials is discussed in terms of their crystal orientations [observed using scanning electron microscopy (SEM) and transmission electron microscopy (TEM)]; the optical characteristics were measured using a microphotoluminescence ( $\mu$ -PL) system. The lumi-

nescence efficiency (measured using the  $\mu$ -PL) and the cathodoluminescence of a single nanostripe were greatly enhanced in comparison to those of conventional thin film MQW structures. In addition, the MQWs embedded in the nanostripe structures were free of dislocations resulting from the interface between the GaN and the substrate, as observed from TEM images.

All samples were grown through MOCVD in a single-wafer Emcore system with a vertical reactor design. We used SiO<sub>2</sub> stripes oriented along the [1 $\bar{1}$ 00] direction as an etching mask to define patterns lithographically on a sapphire substrate. The dimensions of the mask openings and periods were 6 and 8  $\mu$ m, respectively. The sample was wet etched using a H<sub>3</sub>PO<sub>4</sub> base solution at 300 °C for 30 min. Afterward, the sample was dipped into a buffered oxide etch (NH<sub>4</sub>F:HF, 6:1) solution to remove the SiO<sub>2</sub> layers for the following epitaxial growth. The growth parameters of the conventional light-emitting diode on the *c* plane were used for the epitaxial step, including a 30 nm GaN buffer layer, 1  $\mu$ m bulk GaN layer, three pairs of MQWs with 6 nm In<sub>0.2</sub>Ga<sub>0.8</sub>N wells and 16 nm GaN barriers, and a 100 nm GaN capping layer. The surface morphology and microstructure of the as-grown sample were observed using SEM and TEM. A  $\mu$ -PL system pumped by a He-Cd laser was used to study the luminescence in the structure, with the spatial resolution estimated to be approximately 0.7  $\mu$ m. The spatially resolved cathodoluminescence (CL) imaging data were obtained by scanning the SEM over various parts of the samples.

Figure 1(a) provides a schematic diagram of the as-grown sample. For the trapezoidally patterned sapphire, the top width, bottom width, and depth were approximately 450 nm, 6.7  $\mu$ m, and 4  $\mu$ m, respectively. Figure 1(b) displays a top-view SEM image of the as-grown sample. Nanostripes had grown on the top base of the trapezoid.

<sup>a)</sup>Electronic mail: timclu@faculty.nctu.edu.tw

<sup>b)</sup>Electronic mail: hckuo@faculty.nctu.edu.tw

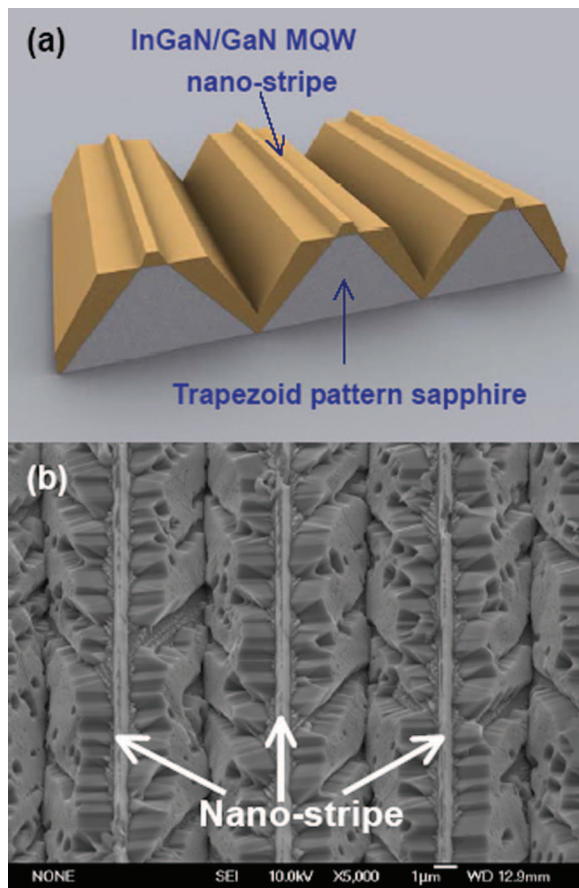


FIG. 1. (a) (Color) Schematic representation of the nanostripe MQWs grown on trapezoidally patterned sapphire substrates. (b) Top-view SEM images of the as-grown sample.

Many V defects and small pits were also widely distributed over the lateral side of the trapezoid. Figure 2(a) presents a typical cross-sectional bright-field TEM image, with different zones labeled I, II, and III. The nanostructure structures existed on top of the trapezoid pattern of the sapphire substrate in zone I. In the TEM images, the MQW structures appeared only in zones I and III. No MQW structures were detected from TEM observation of zone II, indicating that the growth direction might occur only toward the top and lateral facets of the trapezoidally patterned sapphire. According to the diffraction pattern, the GaN layer grown epitaxially on the top face of the trapezoid followed typical  $\{0001\}_{\text{GaN}} \parallel \{0001\}_{\text{sapphire}}$  and  $[11\bar{2}0]_{\text{GaN}} \parallel [1100]_{\text{sapphire}}$  crystallographic relationships, as presented in the inset to Fig. 2(a). The crystallographic relationship of the side facets of the trapezoid differed from that of a typical *c*-plane hexagonal crystallographic geometry, although the crystallographic facets in zone III belonged to the *c* plane. The exact determination of the crystallographic relationship between the GaN and the inclined sapphire face will require the analysis of more than one diffraction pattern from different zone axes; such a study is in progress. Figures 2(b)–2(e) reveal high-resolution TEM images of triple-MQW structures grown on zones I and III, respectively. The thickness of the MQW structure on zone I was larger than that on zone III probably because of the different gas streams caused by the striped patterns on the substrates. From the angle of inclination between the top and side facets of the GaN grown on zone I in this nanostructured structure, we determined that the side facet

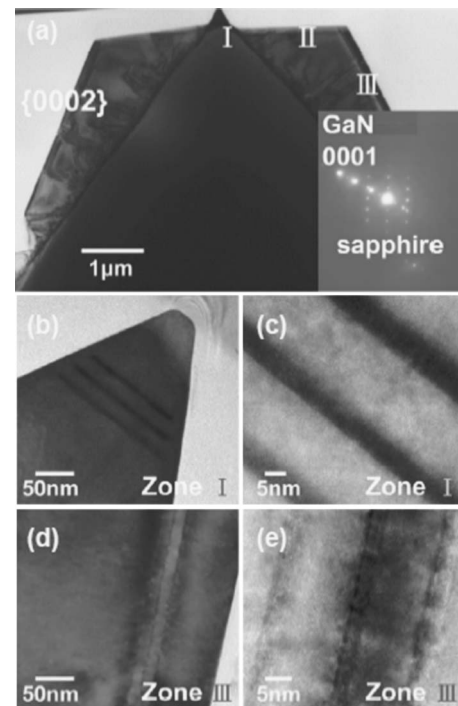


FIG. 2. (a) Cross-sectional TEM image of the trapezoidal structure. The crystalline orientation between the GaN and sapphire in zone II was defined by the diffraction pattern, as indicated in the inset. (b)–(e) High-resolution TEM images (different magnifications) of the MQWs in zones I [(b) and (c)] and III [(d) and (e)].

was a  $\{1\bar{1}02\}$  *r* plane. Moreover, the V-shaped defects commonly observed under conditions of kinetically limited growth of *c*-plane GaN and its alloys<sup>9</sup> are visible in the bottom-left-hand region of the TEM image in Fig. 2(a).

A room temperature  $\mu$ -PL system equipped with a He–Cd laser was used to study the luminescence of the structure. We obtained PL spectra by focusing the laser beam on zones I and III [as labeled in Fig. 2(a)]. Figure 3(a) displays the  $\mu$ -PL results obtained at the different zones of the structure. The PL maximum at zone I appeared at approximately 460 nm, a longer wavelength than that of zone III. According to the TEM images in Figs. 2(b) and 2(d), the widths of the wells were approximately 6 and 2.5 nm for zones I and III, respectively. The longer emission wavelength at zone I relative to that at zone III was due to the wider quantum well size having a weaker quantum confinement effect. In addition, the PL intensity from the single nanostructure in zone I was enhanced up to almost fivefold relative to that of zone III and even relative to that of the regular equal pairs of MQWs in the conventional thin film structures. The much-improved emission efficiency might have arisen from enhanced light extraction efficiency and/or internal quantum efficiency. Because the MQWs were embedded in the trapezoidal nanostructure, the inclination of the large-area emission surface greatly enhanced the light extraction efficiency in comparison with those of conventional flat MQW thin films, where the light emitted only within the cone defined by the angle of total internal reflection. We have used TEM to observe the root of the nanostructure in zone II. Figure 3(b) displays the distribution of edge dislocations in a cross-sectional dark-field TEM image of the nanostructure. In general, edge dislocations often stretch through to the surface to become V defects. This image, however,

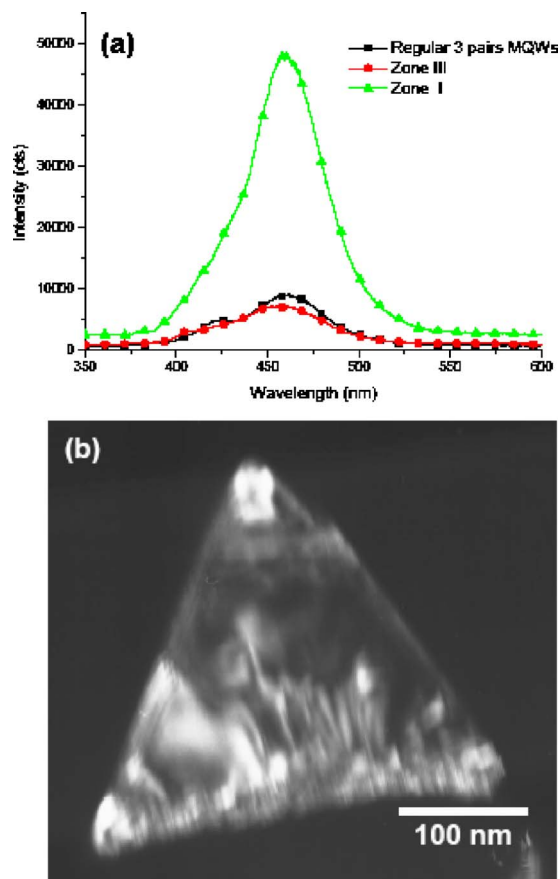


FIG. 3. (Color online) (a) PL spectra recorded at zones I and II and that of a conventional thin film with three pairs of MQWs. (b) Cross-sectional dark-field TEM images of the nanostructures.

indicated that the edge dislocations were terminated in the growth of the bulk GaN layer below the MQW layers. As a result, the nanostructure helped to form MQWs that were free from edge dislocations and facilitated the enhancement of internal quantum efficiency.

Figures 4(a) and 4(b) present spatially resolved cathodoluminescence images recorded using optical filters at 365 and 460 nm, respectively, from above the sample at room temperature. In Fig. 4, zones I and III are the same positions as those defined in Fig. 2(a). The emissions 365 and 460 nm originated mainly from the contributions of the bulk GaN and the InGaN/GaN MQWs. In Fig. 4(a), the optically activated region reveals the locations of the bulk GaN, including some areas between the nanostructures and the top face of the trapezoids; in Fig. 4(b), however, the bright 460 nm MQW emission lines appear at the top of the trapezoids. Meanwhile, zone II also exhibited the MQWs' luminescence, confirming the results of the TEM analysis in Fig. 2. We observe, however, that the luminescence intensity from the MQWs on the nanostructure is stronger than those on both of the lateral regions. Because the distribution of defects and the quality of the crystal can both influence the CL intensity,<sup>10</sup> the high intensity of the emission from the nanostructure again suggests the good epitaxial quality—and lack of V defects—of the MQWs grown on the trapezoidally patterned sapphire substrates.

In summary, we have used MOCVD to fabricate InGaN/GaN MQWs nanostructures on trapezoidally patterned

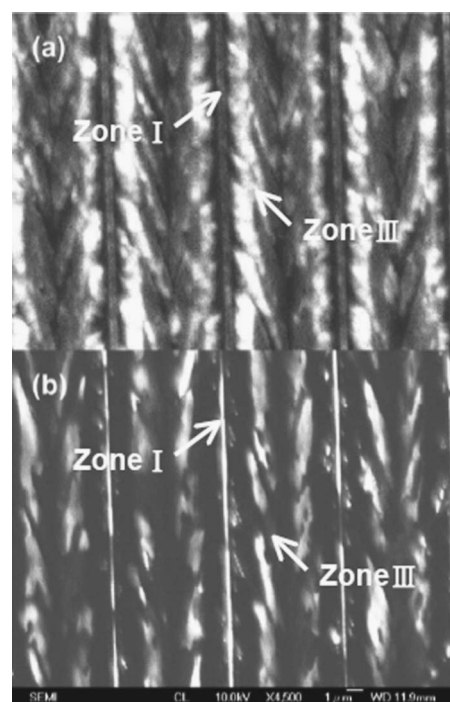


FIG. 4. Monochromatic top view CL images: (a)  $\lambda=365$  nm and (b)  $\lambda=460$  nm.

sapphire substrates. A series of special relations and planes of crystallization were defined by diffraction pattern analysis and TEM observations. The results of  $\mu$ -PL and CL experiments indicate that the intensity of the luminescence from the MQWs embedded in the nanostructure was enhanced up to fivefold relative to those of regular thin film MQWs, probably as a result of much-improved internal and external quantum efficiencies. Therefore, these MQW nanostructure arrays are capable of enhancing luminescence and appear to be suitable for application to the fabrication of high-efficiency light-emitting devices.

The authors would like to thank Professor Y. F. Chen of National Taiwan University for CL support. The study was supported by the MOE ATU program and, in part, by the National Science Council of the Republic of China under Contract Nos. NSC 95-2120-M-009-008, NSC 95-2752-E-009-007-PAE, and NSC 95-2221-E-009-282.

<sup>1</sup>S. Nakamura, *Science* **281**, 956 (1998).

<sup>2</sup>H. Morkoç, S. Strite, G. B. Gao, M. E. Lin, B. Sverdlov, and M. Burns, *J. Appl. Phys.* **76**, 1363 (1994).

<sup>3</sup>F. A. Ponce and D. P. Bour, *Nature (London)* **386**, 351 (1997).

<sup>4</sup>C. Huh, K. S. Lee, E. J. Kang, and S. J. Park, *J. Appl. Phys.* **93**, 9383 (2003).

<sup>5</sup>I. Schnitzer, E. Yablonovitch, C. Caneau, T. J. Gmitter, and A. Scherer, *Appl. Phys. Lett.* **63**, 2174 (1993).

<sup>6</sup>H. M. Kim, Y. H. Cho, H. Lee, S. I. Kim, S. R. Ryu, D. Y. Kim, T. W. Kang, and K. S. Chung, *Nano Lett.* **4**, 1059 (2004).

<sup>7</sup>T. Fujii, Y. Gao, R. Sharma, E. L. Hu, S. P. DenBaars, and S. Nakamura, *Appl. Phys. Lett.* **84**, 855 (2005).

<sup>8</sup>W. K. Wang, S. Y. Huang, K. S. Wen, D. S. Wu, and R. H. Horng, *Appl. Phys. Lett.* **88**, 181113 (2006).

<sup>9</sup>X. Wu, C. Elsass, A. Abare, M. Mack, S. Keller, P. Petroff, S. DenBaars, J. Speck, and S. Rosner, *Appl. Phys. Lett.* **72**, 692 (1998).

<sup>10</sup>B. A. Haskell, T. J. Baker, M. B. McLaurin, F. Wu, P. T. Fini, S. P. DenBaars, J. S. Speck, and S. Nakamura, *Appl. Phys. Lett.* **86**, 111917 (2005).